Eur. Phys. J. Special Topics **224**, 277–288 (2015)

DOI: 10.1140/epjst/e2015-02359-1

THE EUROPEAN PHYSICAL JOURNAL SPECIAL TOPICS

Regular Article

Effect of contact angle hysteresis on breakage of a liquid bridge

H. Chen[1], T. Tang[1,a], and A. Amirfazli[2,b]

[1] Department of Mechanical Engineering, University of Alberta, Edmonton, AB, T6G 2G8, Canada
[2] Department of Mechanical Engineering, York University, Toronto, ON, M3J 1P3, Canada

Received 7 August 2014 / Received in final form 16 February 2015
Published online 8 April 2015

Abstract. In this paper, the importance of considering contact angle hysteresis (CAH) during the process of stretching and breaking a liquid bridge between two solid surfaces is addressed. We clearly show that due to the pinning of contact line at the end of the stretching stage, the contact angle between liquid bridge and surfaces cannot be simply assumed to have a constant value (e.g. receding contact angle, θ_r). Simulation results for stretching a liquid bridge with and without CAH, showed that the contact line pinning can lead to breakage at a larger surface separation and smaller value of pull-off force (F_p). A systematic study about the effect of CAH and contact line pinning on the value of F_p is provided. It is found that when one of the surfaces has a θ_r larger than 90°, F_p decreases with the increase of θ_r on either surface delimiting the bridge. For the cases where θ_r of both surfaces are smaller than 90°, significantly smaller F_p is seen when contact line pinning occurs on both surfaces, as compared to F_p when contact line pinning occurs only on one surface. This smaller F_p is caused by more curved profile and later breakage of liquid bridge.

1 Introduction

Wetting phenomena which is commonly seen in nature and various industrial applications is also of significant interest to academic researchers. The wettability of a surface is usually described by the contact angle, measured within the liquid at the three phase (solid, vapor, and liquid) contact line [1]. In an ideal situation, the contact angle between a specific liquid and a solid surface is a unique value according to the Young's equation [2]. However, due to the roughness and heterogeneity of surfaces, in reality the contact angle does not exhibit a unique value. A range of values can be found between advancing contact angle, θ_a (maximum value of contact angle when liquid advances over a surface); and receding contact angle, θ_r (minimum value of contact angle when liquid recedes over a surface) [3,4]. When the contact line is pinned on the surface, the contact angle can have any value between θ_a and θ_r. The contact angle hysteresis (CAH) is the difference between θ_a and θ_r.

[a] e-mail: ttang1@ualberta.ca
[b] e-mail: alidad2@yorku.ca

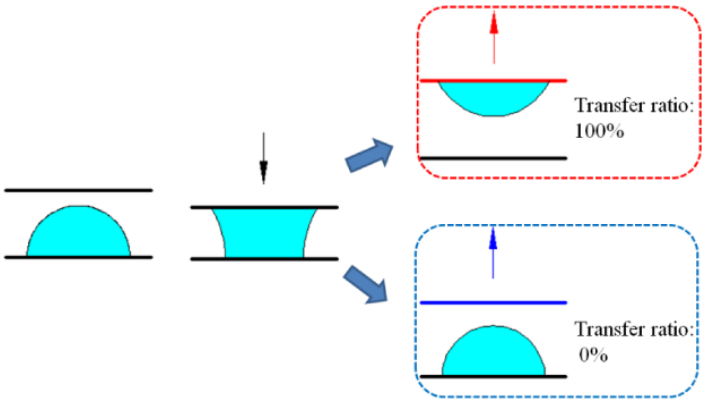

Fig. 1. Process of liquid drop transfer. Two limiting situations with 100% and 0% transfer ratios are shown.

A numbers of previous works have shown that CAH plays a very important role in various types of wetting or dewetting processes, especially the stickiness of surfaces which were shown to be significantly affected by CAH [5–11]. For example, CAH was shown to be one of the governing parameters determining the motion of a drop on a tilted surface [7,8]; CAH can also significantly influence the drop shedding process [9–11]. However, there are very few studies about the effect of CAH on processes involving a liquid bridge, e.g. liquid transfer between two solid surfaces, electronic printing by dispensing a liquid (ink) on polymeric surfaces, wet adhesion systems (of sort seen in nature), etc. In many of these processes a liquid bridge is first formed by an approaching surface to another one where liquid is present (e.g. a sessile drop), see Fig. 1; the liquid bridge then may be compressed, but the final stage usually involves separation of two surfaces and breakage of the liquid bridge (e.g. as seen in off-set printing). When the liquid bridge breaks the volume of the drop is divided between the lower and upper surfaces. In the limiting situation where no liquid from the lower surface is transferred to the upper surface (see Fig. 1), it is said that the transfer ratio is zero. The transfer ratio has a value of one, if all of the liquid from the lower surface is transferred to the upper surface when liquid bridge breaks.

In this study a typical process of quasi-static compression and stretching of a liquid bridge between two surfaces will be considered. A number of works have been done to understand this process [12–16]. In most of the previous literature, the value of contact angle was simply assumed as a constant (value of equilibrium contact angle, or receding contact angle) during the whole process [14–16]. Such assumption also implicitly means that the contact line continuously recedes to shrink the contact area between one or both surfaces delimiting the liquid bridge, i.e. contact line will not be pinned. However, in various recent studies it was observed that the contact angles of the upper and/or lower surfaces with the liquid bridge during compression and stretching is not constant, i.e. θ_a in most of compressing stage, and θ_r in most of stretching stage [17–19]. Contact line pinning can be observed when the contact angle changes between θ_a and θ_r.

Two recent studies [20,21] showed that the transfer ratio for quasi-static liquid transfer is strongly depended on the difference between the receding contact angles of the two surfaces. In fact, the key mechanism [21] which governs the transfer ratio is the pinning of contact line (caused by CAH) before the pull-off (final breakage) of the liquid bridge. It was found that the contact angle did not always stay at the receding value, but could increase at the end of the stretching stage, due to contact line pinning. Therefore, it was argued [21], the presumption that the receding contact

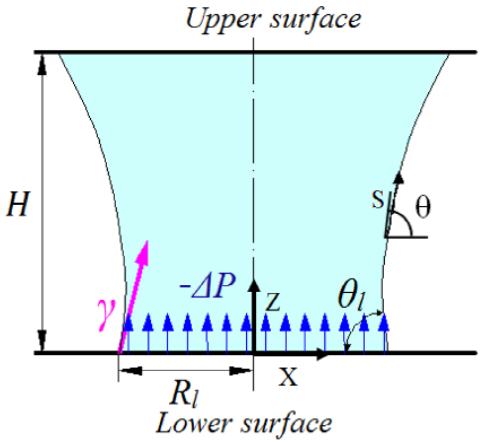

Fig. 2. Schematic of a liquid bridge between two solid surfaces. R_l and θ_l are the contact radius and contact angle on the lower surface. H is the distance between the two surfaces, and γ is the surface tension of liquid.

angle will be always observed when liquid bridge breaks is not warranted. Pinning of the contact line will not only change the contact angle and hence the associate surface tension force, but also the shape of the liquid bridge leading to a change in the Laplace pressure (ΔP). Since both surface tension force and Laplace pressure determine the force experienced by the liquid bridge at either of the two delimiting surfaces (see Fig. 2), it is important and necessary to consider the effect of CAH on the adhesion force when liquid bridge breaks (or pull-off force).

In this paper we present a systematic study about how the pinning of contact line at the end of the stretching stage influences the value of pull-off force (F_p). Different from [21] which studied the mechanism of quasi-static liquid transfer (e.g. the role of pinned contact line), this work is focused on investigating the effect of CAH on the pull-off force and address questions such as: how does F_p change with the contact angles and CAH of the surfaces? How does such change correlate with the surface separation and geometry of the liquid bridge when it breaks, and how may one make use of the results and modulate F_p via CAH? These questions were addressed by firstly, demonstrating the importance of CAH in the stretching stage by comparing the process of stretching a liquid bridge with CAH and without CAH. Secondly, it will be shown how pinning of contact line at the end of stretching stage influences the value of pull-off force.

2 Methods

The focus of this study is on a liquid bridge formed between two surfaces that are much larger than the contact area between the liquid bridge and either of the surfaces. Liquid bridge formed between ten different lower surfaces (for wettability data see Table 1) and one Poly(methyl methacrylate) upper surface (PMMA(1), θ_a: 72.6°θ_r: 60.3°) were studied experimentally for a 2 μl water drop which has the surface tension and density of 72.8 mN/m and 9.98 g/ml respectively at 20°C. With such a small liquid drop, the value of Bond Number ($Bo = \frac{\rho g R^2}{\gamma}$, where R is a characteristic length, taken to be the average of the contact radii on the acceptor and donor surfaces) is on the order of 10^{-2}, which indicates that gravity is negligible for the systems we studied. The surfaces were fabricated as described in [22]. In each experiment, the upper surface

Table 1. Wetting properties of the lower surfaces with water. Sessile drop method was used in the measurement of contact angle. For each surfaces, measurements for contact angle were conducted at three different locations. The shown data are the average value and standard deviation of the three measurements.

Name of surface	θ_a (degree)	θ_r (degree)
Silicon	55.1 ± 0.67	45.7 ± 1.23
PMMA(2)	71.9 ± 0.70	52.7 ± 1.54
PMMA(3)	72.8 ± 0.93	57.9 ± 0.86
Polystyrene & PMMA Blend (1)	73.0 ± 0.82	59.7 ± 0.97
Polystyrene & PMMA Blend (2)	79.4 ± 0.73	63.9 ± 0.94
Polystyrene (1)	88.6 ± 1.43	66.0 ± 1.27
Poly (ethyl methacrylate)	77.6 ± 0.79	68.2 ± 0.94
Polystyrene (2)	91.8 ± 1.30	75.3 ± 0.87
Octadecyltrichlorosilane Treated	111.1 ± 1.33	98.2 ± 0.89
Teflon AF	126.4 ± 1.30	116.4 ± 0.93

was stretched at a low speed of 0.005 mm/s to ensure the quasi-static condition (the experimental setup used was similar to one in our earlier study described in [21]). The pull-off forces were recorded by a force cell (resolution of 0.005 mN) attached to the lower surface. All experiments were performed under well controlled ambient conditions (pressure, temperature and relative humidity).

In addition to the experiments, a theoretical model developed earlier by us was used to simulate the quasi-static stretching of a liquid bridge between two surfaces with CAH. As shown in Fig. 2, neglecting the effect of gravity, the equilibrium profile of the liquid bridge can be described by the following equations [17,23]

$$\frac{dX}{dS} = \cos\theta \tag{1}$$

$$\frac{dZ}{dS} = \sin\theta \tag{2}$$

$$\frac{d\theta}{dS} = \frac{\Delta P}{\gamma} - \frac{\sin\theta}{X} \tag{3}$$

where X and Z are the coordinates of the axisymmetric liquid bridge, S is the arc length measured from the contact point of the liquid with the lower surface, and θ is the angle between the local tangent of the liquid surface and the horizontal axis. Given the surface separation H and assuming the volume of the liquid is conserved, the shape of the liquid bridge can be obtained by solving Eqs. (1)–(3) with boundary conditions that specify either contact radius or contact angle on each of the two surfaces. The shooting method was used to find the solution in an iterative manner [17]. Once the profile of the liquid bridge is obtained, the adhesion force can be calculated based on ΔP, contact angle and contact radius on either upper or lower surface. Taking the lower surface for example, the magnitude of adhesion force can be calculated as:

$$F = 2\gamma\pi R_l \sin\theta_l - \pi R_l^2 \Delta P. \tag{4}$$

The vertical adhesion force consists of two terms, the first due to surface tension force and the second due to Laplace pressure. With this model, the geometry of the liquid bridge during the stretching process was monitored; hence the contact angle, contact radius as well as the adhesion force on both surfaces can be obtained. This theoretical model is based on the assumption of equilibrium. When H becomes larger

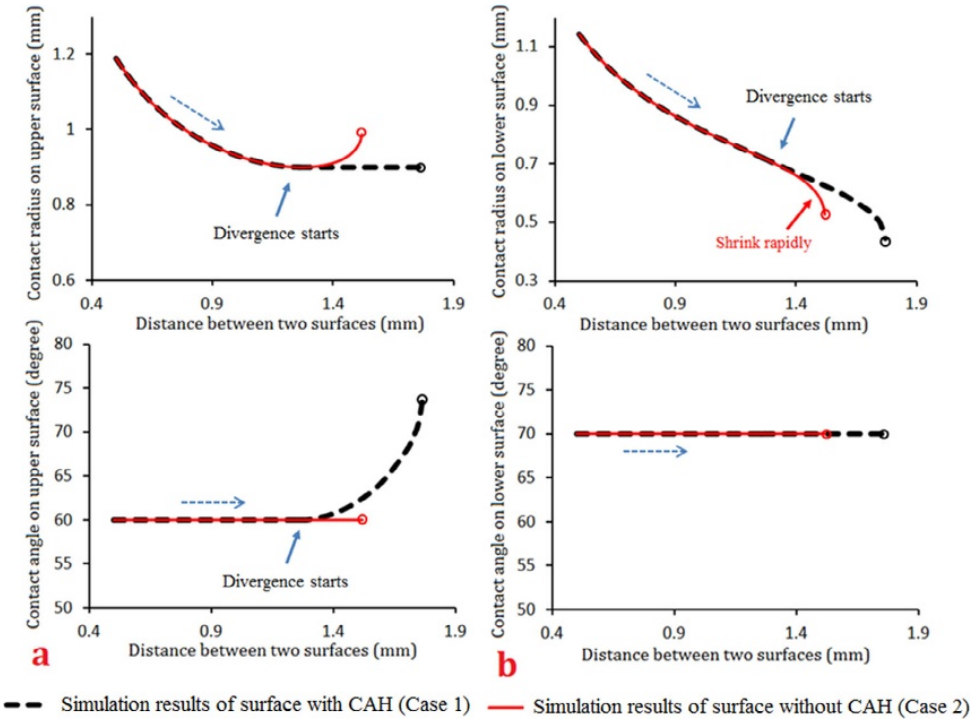

Fig. 3. Evolution of contact radius and contact angle for Cases 1 and 2; (a) the upper surface; (b) the lower surface. Hollow circles denote the points at which the liquid bridge breaks.

than a certain value (the separation where liquid bridge breaks, denoted as $H_{\max}$), the liquid bridge becomes unstable, and no convergence solutions can be found from the model. The pull-off force F_p evaluated from the model is based on the last equilibrium solution, obtained at $H \approx H_{\max}$.

3 Results and discussion

The first system simulated (denoted as Case 1) is a liquid bridge between a lower surface (θ_a: 90°, θ_r: 70°) and an upper surface (θ_a: 80°, θ_r: 60°). The initial separation (H_{min}) between the two surfaces was set to be 0.5 mm, and the initial contact angle was set to be the receding contact angle for each of the surfaces. In order to demonstrate the importance of CAH, another simulation of stretching the liquid bridge was done, but this time without CAH consideration (Case 2). In Case 2, the contact angle of the upper and lower surfaces was set as 60° and 70°, respectively, which are the values of the receding contact angles in Case 1 (this was done to represent what has been mainly proposed in the literature during the stretching phase, as discussed earlier).

The evolution of the contact radii and contact angles of the two cases are shown in Fig. 3. It can be seen that in the early stage of the stretching process ($H < 1.27$ mm), because the contact angles of both cases are at the receding values, the curves of Cases 1 and 2 overlap. However, after H increases to 1.27 mm, the two contact radius curves diverge. Consider first the upper surface, shown in Fig. 3a. In Case 1 where CAH is present, instead of remaining at the receding value, the contact angle starts

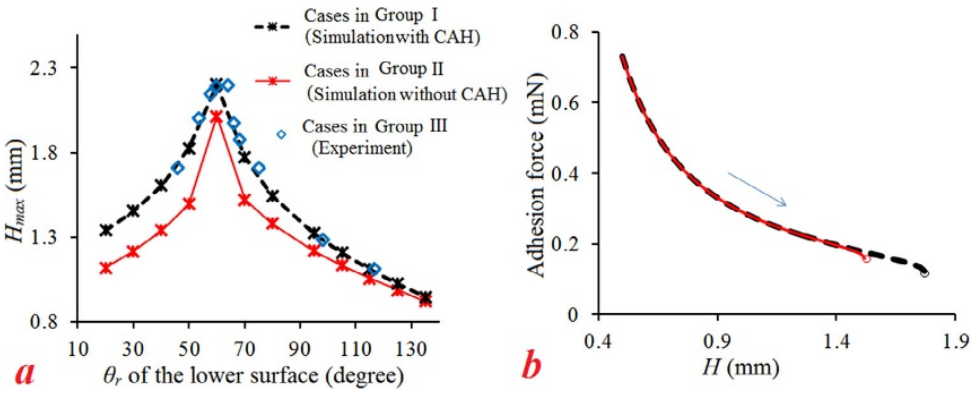

Fig. 4. (a) Value of H_{max} versus θ_r for the lower surface in simulations (Groups I/II) and experiments (Group III). Lines are to guide the eyes. (b) Evolution of the adhesion force for Cases 1 and 2. Hollow circles mark the points at which the liquid bridge breaks.

to increase, while the contact radius is pinned at 0.90 mm during the rest of the stretching stage. However, for Case 2 where CAH is absent, the contact angle stays constant while the contact line starts to expand after H reaches 1.27 mm. For the lower surface, shown in Fig. 3b, the contact angles on both surfaces stay at the receding value and no contact line pinning is observed. However, due to the distinct behavior of contact angle/contact line on the upper surface, the contact radius on the lower surface also behaves differently near the breaking point (where pull-off force is registered). For Case 2, since the volume of the liquid is constant, associated with the expansion of contact radius on the upper surface, the contact radius on the lower surface shrinks rapidly. On the contrary, the contact line pinning on the upper surface in Case 1 allows the contact radius on the lower surface to decrease at a slower rate. As a result, the liquid bridge in Case 1 breaks at a much larger H value than in Case 2. Specifically $H_{\max} = 1.77$ mm in Case 1, a 16.4% increase compared with Case 2 where $H_{\max} = 1.52$ mm.

To further confirm that CAH leads to larger H_{max}, two sets of simulations and one set of experiments were performed. Both simulation groups have the same set of lower surfaces with their receding contact angles varying from 20° to 135°. The difference between the two groups of simulations lies in the upper surface. In the first simulation group (Group I), the upper surface has CAH (θ_a: 80°, θ_r: 60°) and hence contact line pinning can occur on both upper and lower surfaces. In the second group (Group II), the contact angle of the upper surface is fixed at 60° (same as θ_r of upper surface in Group I) without CAH, and therefore contact line pinning can only occur on the lower surface. Experimental measurements (Group III) of liquid transfer from different lower surfaces to a fixed upper surface were also finished. The upper surface used in the experiment has $\theta_a = 72.6°$ and $\theta_r = 60.3°$, the latter almost the same as θ_r of the upper surface used in the simulations. Data on H_{max} versus θ_r of the lower surface obtained from all three groups are plotted in Fig. 4a. It can be seen that due to the absence of CAH on the upper surface, the results from Group II are very different from those in Group I and Group III. The experimental data (Group III) fall nicely onto the curve generated from simulation Group I (with CAH on both surfaces) but deviate significantly from Group II, emphasizing the importance of considering CAH for any realistic system. At the same θ_r of the lower surface, the value of $H_{\max}$ in Group I is larger than those in Group II, confirming that the pinning of contact line at the end of stretching stage, in general, causes an increase in $H_{\max}$.

The adhesion force between the liquid and surfaces is influenced by the geometry of the liquid bridge profile, so it can be affected by CAH. The evolution of the

adhesion forces in the two cases simulated in Fig. 3 are shown in Fig. 4b. It can be seen that the value of the adhesion force decreases with the increase of H. Because the liquid bridge in Case 1 breaks at larger H_{max}, compared with Case 2, Case 1 has a smaller value of F_p. However, if we compare the adhesion force between the two cases at the same H, the adhesion force in Case 1 is the same as in Case 2 when $H < 1.27$ mm (before divergence starts), and slightly larger than in Case 2 when $1.27\,\text{mm} < H < 1.52\,\text{mm}$ (after divergence but before breakage in Case 2).

Having understood the importance of CAH in the stretching of a liquid bridge, the following discussion is focused on how CAH and the pinning of contact line affect the value of F_p. In [21], it was shown that depending on the receding contact angles of the two surfaces, the pinning of the contact line at the end of stretching stage can occur only on one surface when the receding angle of the two surfaces are very different, or on both surfaces, when the receding angle of the two surfaces are similar.

The pull-off force data from Group I (simulation) and Group III (experiment) are plotted in Fig. 5a versus θ_r of the lower surface. Two observations can be made from the plot. First, when the lower surface has a large receding contact angle ($> 70°$, for this group), F_p clearly decreases with the increase of the receding contact angle. However, when the receding contact angle of the lower surface is small ($< 70°$), no monotonic relation between F_p and the receding contact angle can be found. In addition, there appears to be a local minimum in the F_p curve, located about θ_r of the lower surface $= 60°$, which is near the receding contact angle of the upper surface. For example, from Group I, F_p at 60° receding contact angle of lower surface (0.0835 mN) is significantly smaller than F_p at both 70° (0.1219 mN) and 50° (0.1210 mN).

To further explore and understand the observations in Fig. 5a, we simulated six more groups of liquid transfer. In each group, the receding contact angle of upper surface is fixed (see Fig. 5b) and different lower surfaces were used. The results for F_p are shown in Fig. 5b versus θ_r of the lower surface. Each curve in Fig. 5b connects F_p data associated with the same upper surface. Similar to Fig. 5a, for each curve, when θ_r of the lower surface is large ($> 90°$ for all the groups), F_p decreases with an increasing value of θ_r on the lower surface. Furthermore, comparison among the different curves shows that F_p also decreases with increasing θ_r on the upper surface. No monotonic relation between F_p and θ_r of either surface can be found when θ_r of the lower surface becomes small ($< 90°$). However, by examining θ_r of the two surfaces for the cases with significantly smaller F_p, it was found that all of these cases have similar values of θ_r on the two surfaces. Furthermore, due to the similar θ_r values, contact line pinning takes place on both lower and upper surfaces at the end of the stretching stage (pointing to the importance of considering CAH when analyzing a liquid bridge).

Since the adhesion force is influenced by the shape of the liquid bridge, the profiles of the liquid bridge near the breakage point for all the data shown in Fig. 5 were examined to understand how the occurrence of contact line pinning affects F_p. Figure 6 shows the profiles of three liquid bridges near pull-off obtained from the simulations. All three liquid bridges have the same θ_r on the upper surface (60°) but different θ_r on the lower surface (liquid bridge ①: 50°, liquid bridge ②: 60° and liquid bridge ③: 70°). The different value of θ_r on the lower surfaces results in completely different contact line pinning behaviors at the end of stretching stage (liquid bridge ①: only on the lower surface; liquid bridge ②: on both surfaces; and liquid bridge ③: only on the upper surface). At the end of the stretching stage, the liquid has a tendency to stay near the surface which has a smaller contact angle, and hence contact line pinning on that surface can be observed. The more different the receding contact angles of the two surfaces, the stronger this tendency will be, and contact line pinning is more

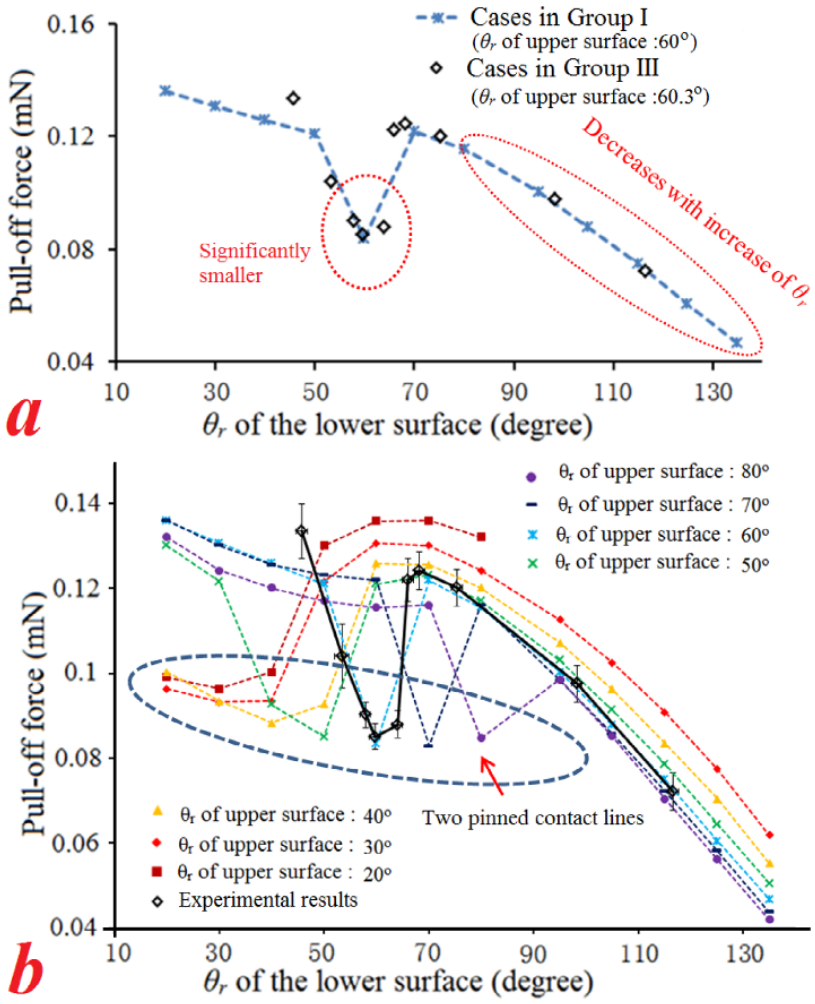

Fig. 5. (a) Value of pull-off forces versus θ_r of the lower surface, data from simulations (Group I) and experiments (Group III). (b) Value of pull-off forces versus θ_r of the two surfaces of all the cases. Lines are to guide the eyes.

expected to occur only on one surface (with smaller θ_r). It can be seen that compared with the liquid bridges with only one pinned contact line, the one with two pinned contact lines has a more curved profile when it breaks. Due to the larger curvature, the value of $-\Delta P$ of bridge ② ($-129.5\,\mathrm{N/m^2}$) is much smaller than $-\Delta P$ of bridges ① ($-98\,\mathrm{N/m^2}$) and ③($-106.7\,\mathrm{N/m^2}$). From the Eq. (4), the value of adhesion force is positively related to $-\Delta P$. Therefore, the adhesion force between the liquid and surface of the cases that have two pinning contact lines are smaller than the cases where only one contact line is pinned.

Another reason contributing to the smaller pull-off force associated with two pinned contact lines is the later breakage (larger H_{max}) of the liquid bridge. It has been observed in Fig. 4b that compared with situations without CAH, contact line pinning delays breakage and reduces F_p. It can also be noticed from Fig. 6 that liquid bridge ② has a larger $H_{\max}$(②: $H_{\max} = 2.20\,\mathrm{mm}$, ①:$H_{\max} = 1.82\,\mathrm{mm}$ and ③ $H_{\max} = 1.77\,\mathrm{mm}$). Since F_p is the adhesion force measured at $H_{\max}$, it is of interest

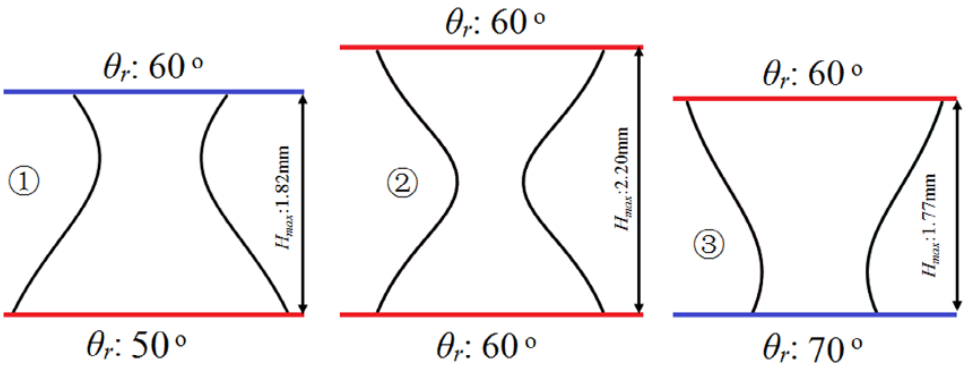

Fig. 6. Profiles of liquid bridge before it breaks obtained from simulations; Red: surface with contact line pinning; Blue: surface without contact line pinning. The occurrences of contact line pinning are: ① only on lower surface; ② on both surfaces; ③ only on upper surface.

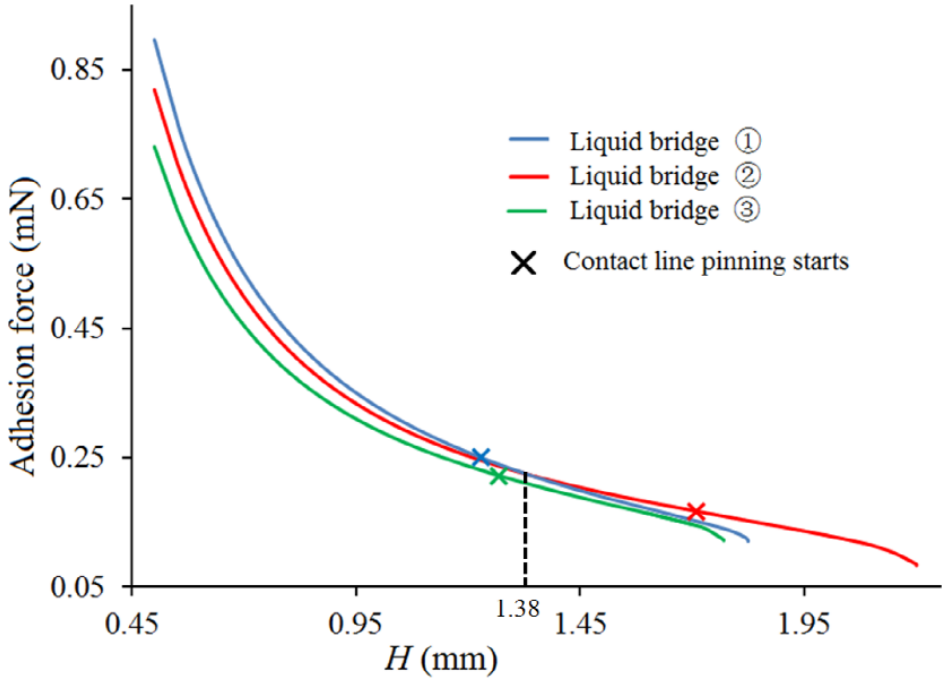

Fig. 7. Evolution of adhesion force for the liquid bridge ①, ② and ③.

to compare the evolutions of the adhesion forces during stretching the three liquid bridges, which are shown in Fig. 7. It is clear that the curve for liquid bridge ② extends to a much larger separation, leading to smaller value of F_p. On the other hand, although bridge ② has the smallest F_p, at the same H its adhesion force is not the smallest among these three bridges. When H is larger than 1.38 mm, bridge ② in fact has the largest adhesion force compared with the other two. This is similar to observation in Fig. 4b where the introduction of CAH does not cause reduction in the adhesion force at the same surface separation.

Summarized from the discussion, the contact lines of liquid bridge may become pinned when CAH is present during the process of stretching. Such phenomenon of

contact line pinning alters significantly both the shape and stability of the liquid bridge. Due to the effect of CAH, it is shown that liquid bridges with free moving contact lines may behave as liquid bridge whose contact lines are forced (e.g. due to geometric constraints) to be pinned. For example, three of our experimental cases (water transfer from PMMA (3), Polystyrene & PMMA Blend (1), and Polystyrene & PMMA Blend (2) to PMMA (1)) were found to have two pinned contact lines at the end of the stretching stage. We compared the these three cases with two previous studies [25,26] which considered surfaces that had small areas and assumed that the liquid bridge had pinned contact lines on the edges of both surfaces. Good agreements were found (for detailed comparison, see Appendix).

Results from this work can be useful to practical applications involving liquid bridges. The finding that in the presence of CAH liquid bridges break at a large separation distance, especially when both contact lines are pinned, can be useful in understanding wet adhesion systems. Compared with dry adhesion, wet adhesion usually can take effect at larger scales due to the existence of liquid bridges [24]. As shown in this study, the pinning of contact line due to CAH, especially on both surfaces, can significantly increases H_{max}, the effective interaction range, without causing great changes in the adhesion force at the same separation. Both features are desirable for wet adhesion systems, and can be achieved simultaneously by CAH-induced contact line pinning. The occurrence of contact line pinning can also be used to modulate the pull-off force. For instance, depending on the receding contact angles of the two surfaces, the value of F_p can be decreased in two different ways. If one of the receding contact angles is very large ($> 90°$), a smaller F_p can be obtained by increasing θ_r of either surface. If the θ_r values are smaller than 90° for both surfaces, the way to decrease the pull-off force is to use two surfaces with similar values of θ_r. This will allow contact line pinning to occur on both surfaces in the end of the stretching stage, so as to achieve a smaller F_p.

4 Conclusion

In this paper, we clearly demonstrate that due to the pinning of the contact line at the end of the stretching stage, the contact angle between a liquid bridge and surfaces cannot be simply assumed to have a constant value. Contact line pinning can result in a larger $H_{\max}$, and smaller F_p for liquid transfer. A systematic study about the effect of CAH and the occurrence of contact line pinning on the value of F_p and $H_{\max}$ was provided. It is found that when one of the surfaces has a receding contact angle larger than 90°, F_p decreases with the increase of the receding contact angle on either surface. For the cases where θ_r of both surfaces are smaller than 90°, significantly smaller F_p is seen when contact line pinning occurs on both surfaces, as compared to F_p when contact line pinning occurs only on one of the surfaces. This smaller value of F_p is caused by more curved profile and larger $H_{\max}$ of liquid bridge.

We thank Xerox Foundation and Canada Research Chair Program (T. Tang) for their financial support.

Appendix

Ref. [25] cited in the main texts studied the stability of a liquid bridge between surfaces that had small areas and assumed that the liquid bridge had pinned contact lines on the edges of both surfaces. Four dimensionless parameters were introduced to

Table A1. Value of K, V, Λ and B of the three experimental cases results.

Name of donor surface	K	V	Λ	B
PMMA (3)	0.858	0.467	1.345	−0.0860
Polystyrene & PMMA Blend (1)	0.930	0.458	1.374	−0.0859
Polystyrene & PMMA Blend (2)	0.871	0.477	1.408	0.0826

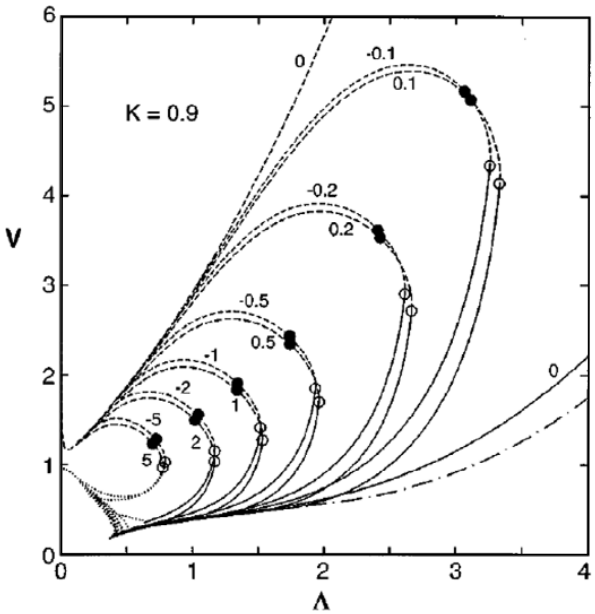

Fig. A1. Influence of positive and negative Bond number on the stability limits with K = 0.9. Numbers on curves denote values of B. Solid (dashed) lines correspond to states critical to axisymmetric (nonaxisymmetric) perturbations. Dotted lines represent states with limiting surfaces, and the dot–dash line is the minimum volume stability limit for zero-gravity bridges between equal disks (K = 1, B = 0).

describe the stability of the liquid bridge: K (ratio of smaller contact radius over the larger contact radius), V ($v/2\pi R^2 H_{\max}$, where v is the actual volume of liquid, $H_{\max}$ is the separation where the liquid bridge becomes unstable, and R is the average of the contact radii on the acceptor and donor surfaces), Λ ($H_{\max}/2R$) and B (Bond Number, positive if the gravity is directed toward the smaller surface, and negative if the gravity is directed toward the larger surface). The values of these four dimensionless numbers of three experimental cases in our study (water transfer from PMMA (3), Polystyrene & PMMA Blend (1), and Polystyrene & PMMA Blend (2) to PMMA (1)) where two pinned contact lines are present due to CAH are shown in Table A1. All of the three cases have similar values for the four dimensionless numbers: B is close to zero, K is near 0.9, Λ is around 1.4 and V is around 1.46. Consulting with Fig. 2a in Ref. [25] where K = 0.9 (shown as Fig. A1 here) and consider the curve that corresponds to B = 0, it can be seen that the values of Λ and V from our experiments fall on the curve. This confirms that a liquid bridge without constrained contact lines can behave like a liquid bridge whose contact lines are constrained by finite surfaces, due to contact line pinning caused by CAH.

References

1. P.G. de Gennes, Rev. Mod. Phys. **57**, 827 (1985)
2. T. Young, Philos. Trans. R. Soc. London **95**, 65 (1805)
3. C.N.C. Lam, R. Wu, D. Li, M.L. Hair, A.W. Neumann, Adv. Colloid Interface Sci. **96**, 169 (2002)
4. R.H. Dettre, R.E. Johnson Jr. Adv. Chem. Ser. **43**, 112 (1964)
5. P. Roura, J. Fort, Phy. Rev. E **64**, 011601 (2001)
6. E. Pierce, F.J. Carmona, A. Amirfazli, Colloids Surf. A **323**, 73 (2008)
7. W. Konrad, M. Ebner, C. Traiser, A. Roth-Nebelsick, Pure Appl. Geophys. **169**, 835 (2012)
8. D. Qurere, Annual Rev. Mater. Res. **38**, 71 (2008)
9. J. Wu, J. Xia, W. Lei, Bao-ping Wang, Scientific Reports **3**, 3268 (2013)
10. L.W. Schwartz, Langmuir **14**, 3440 (1998)
11. A.J.B. Milne, A. Amirfazli, Langmuir **25**(24), 14155 (2009)
12. A.V. Chadov, E.D. Yakhnin, Kolloidn. Zh. **41**, 817 (1979)
13. S. Dodds, M.S. Carvalho, S. Kumar, Phy. Fluids **21**, 092103 (2009)
14. H.W. Kang, H.J. Sung, T.-M. Lee, D.-S. Kim, C.-J. Kim, J. Micromech. Microeng. **19**, 015025 (2009)
15. E. Cheung, M. Sitti, J. Adhesion Sci. Tech. **22**, 569 (2008)
16. M.A. Fortes, J. Colloid Interface Sci. **88**, 2 (1982)
17. H. Chen, A. Amirfazli, T. Tang, Langmuir **29**, 3310 (2013)
18. E.J. De Souza, L. Gao, T.J. McCarthy, E. Arzt, A.J. Crosby, Langmuir **24**(4), 1391 (2008)
19. S.-J. Hong, T.-H. Chou, S.H. Chan, Y.-J. Sheng, H.-K. Tsao, Langmuir **28**, 5606 (2012)
20. B. Samuel, H. Zhao, K.-Y. Law, J. Phys. Chem. C **115**, 14852 (2011)
21. H. Chen, T. Tang, A. Amirfazli, Soft Matt. **10**, 2503 (2014)
22. H. Chen, T. Tang, A. Amirfazli, Colloids Surf. A **408**, 17 (2012)
23. J. Qian, H. Gao, Acta Biomater. **2**, 51 (2006)
24. B.N.J. Persson, J. Phys.: Condens. Matt. **19**, 376110 (2007)
25. L.V. Slobozhanin, J.I.D. Alexander, Phys. Fluids **10**, 2473 (1998)
26. J.M. Perales, J. Meseguer, J. Crystal Growth **110**, 855 (1991)